Real-Time 2nd-order Gaze Metrics

Andrew T. Duchowski[1], Krzysztof Krejtz[2], and Iza Krejtz[2]

[1] Clemson University, Clemson SC, USA duchowski@clemson.edu
https://clemson.edu
[2] SWPS University, Warsaw, Poland [kkrejtz, ikrejtz]@swps.edu.pl
https://swps.edu.pl

Abstract. Real-time implementation of gaze-based 2nd order metrics is given, including computation of the $\mathcal{K}$ coefficient and gaze transition entropy. Innovations include strategies for real-time update of both metrics, dependent on instantaneous real-time binary gaze classification (saccades or fixations), normalization of the $\mathcal{K}$ coefficient, and correction of gaze transition entropy so that special cases are better handled, including gaze fixating a specific Areas Of Interest (AOI) for a prolonged period, or gaze falling outside of all defined AOIs. The resulting implementations are sensitive to the length of the history buffer maintained for either computation, but both produce intuitively interpretable estimates of gaze behavior. Both metrics are implemented in a *context-free* manner allowing for future use in eye-tracking systems that do not possess scene cameras and where there is a need for instantaneous gaze-based biometric measures, e.g., captured over the course of a day.

Keywords: Eye tracking · Metrics · Real-time implementation

1 Introduction

Well-known so-called 1st order gaze-based metrics include numbers of fixations and fixation durations, often employed as a proxy for cognitive function, dating back to Just and Carpenter's *eye-mind assumption* [9], stating that whatever is fixated implies visual inspection via cognitive processing. Krejtz et al. introduced two key 2nd order metrics, namely gaze-based transition entropy [12] and the $\mathcal{K}$ coefficient [13] along with its visualization [5]. These metrics have been widely adopted, providing reproducible results in numerous applications, including aviation [2], transportation [18], learning [14], packaging usability [4], cartographic visual exploration [11], and many others (see Negi and Mitra [14] in particular for a summary of literature based on ambient/focal fixation classification).

Since then, there has been growing demand for implementation of these metrics as real-time indicators of assumed cognitive function they are considered to represent, e.g., ambient/focal visual scanning as given by the $\mathcal{K}$ coefficient or predictability of scanning behavior as given by gaze entropy.

Only a single example of real-time second-order metric implementation has appeared thus far, to the best of our knowledge. Namely, Abeysinghe et al. [1] evaluated a time-windowed implementation of $\mathcal{K}$. Yielding negative values, ${}^{w}\mathcal{K}$

showed entirely ambient viewing behavior of participants during a puzzle-solving task, where the ^{w} superscript denotes group-based windowed computation of $\mathcal{K}$ (see Sec. 2 below).

In this paper, details of real-time implementation of gaze entropy and $\mathcal{K}$ are given, with notes on sensitivity of the algorithms to real-time parameters.

2 Implementation

Both real-time implementations of gaze entropy and $\mathcal{K}$ extend prior work developed for offline analysis [12,13]. Both metrics have generally been used to analyze recorded eye movements on a per-trial basis, i.e., $\mathcal{K}$ or entropy computed over usually short trials conducted on the order of several minutes.

In the first case, $\mathcal{K}$ relies on a fairly straightforward comparison of fixation duration and saccade amplitude. This can clearly be implemented in real-time so long as eye movements can be classified as either fixation or saccade in real time. Specifically, given the next incoming gaze point sample $g_i = (x, y, t)$, this point can generally be classified via a digital filter such as the commonly used differential filter developed by Savitzky and Golay [16] (see Schafer [17] for an in-depth explanation of its design). Used in this way as a differential filter leads to the velocity-threshold identification (I-VT) event detection described early on by Salvucci and Goldberg [15], characterized as a "saccade picker" by Karn [10].

Although binary classification of real-time gaze into saccades and fixations is overly simplistic and omits classification of smooth pursuits or the Vestibulo-Ocular Response (VOR), it does lead to a fairly useful event table with two states, yielding four possible event transitions: (1) saccade → saccade, (2) saccade → fixation, (3) fixation → fixation, and (4) fixation → saccade. Various algorithmic bookkeeping operations can be performed during event state transitions, e.g., during fixation onset (2) or fixation termination (4).

Similarly, in the second case, gaze entropy also relies on the decision of whether transitions between specific Areas Of Interest (AOIs) are recorded based on fixation-to-fixation transitions, or more instantaneously on real-time gaze g_i irrespective of its classification.

In both cases, computation of $\mathcal{K}$ and entropy relies not only on the length of the differential filter but also on the length of the buffer over which either metric is computed. $\mathcal{K}$ relies on estimation of recent means of fixation duration and saccade amplitude. This will depend on the length of buffer of recent events. Similarly, entropy depends on the number of transitions which are used to construct the transition matrix composed of observed transition probabilities.

The longer the buffer, the longer the *memory* of the system. This will necessarily be reflected in response of the system to its estimation of $\mathcal{K}$ or entropy.

2.1 Ambient/Focal $\mathcal{K}$ Coefficient

The $\mathcal{K}$ coefficient is typically computed by Eq. (1),

$$\mathcal{K}_i = \frac{d_i - \mu_d}{\sigma_d} - \frac{a_{i-1} - \mu_a}{\sigma_a} \tag{1}$$

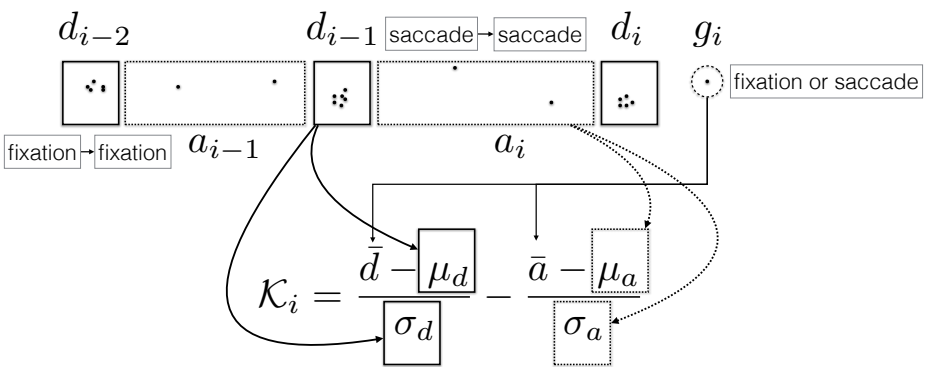

Fig. 1: Real-time computation of $\mathcal{K}$: the top part of the figure shows the temporal accumulation of gaze points g_i classified as either part of fixation durations $\{\ldots, d_{i-1}, d_i\}$ or saccade amplitudes $\{\ldots, a_{i-1}, a_i\}$. Given a new point g_i, it is either accumulated into $\bar{d}$ as the difference between timestamps $\Delta t = g_{i_t} - g_{i-1_t}$ between the current and last points, or it is accumulated into $\bar{a}$ as the difference in position $\Delta\theta = \|g_i, g_{i-1}\|$ converted to degrees visual angle.

where d_i is the current (i^{th}) fixation duration and a_{i-1} is the preceding saccade amplitude. The idea behind $\mathcal{K}$ is to compute the (instantaneous) ratio of fixation duration to saccade amplitude, yielding positive values of $\mathcal{K}$ during focal fixations (long duration minus short saccades) and vice-versa. Due to differing units of time and distance, $\mathcal{K}$ is normalized using z-score standardization, with μ_a, μ_d and σ_a, σ_d the means and variances of previously observed fixation durations and saccade amplitudes, respectively, over time, i.e., typically the duration of an entire trial performed by participants when $\mathcal{K}$ is computed offline.

Real-time implementation of $\mathcal{K}$ is conceptually tied to completion of any given fixation, i.e., transition from fixation to saccade, e.g., as detected by velocity-based filtering. Moreover, one can compute a windowed version of $\mathcal{K}$ over the n few fixations, similarly to the implementation of Abeysinghe et al. [1], who proposed ${}^{w}\mathcal{K}$ as given by Eq. (2), where $\mu_{w,\cdot}$ and $\sigma_{w,\cdot}$ are the mean and variance defined over a window instead of over the duration of a trial.

$$ {}^{w}\mathcal{K}_i = \frac{1}{|w|} \sum_{i \in w} {}^{w}\mathcal{K}_i; \quad {}^{w}\mathcal{K}_i = \frac{d_i - \mu_{w,d}}{\sigma_{w,d}} - \frac{a_{i-1} - \mu_{w,a}}{\sigma_{w,a}} \tag{2} $$

However, Abeysinghe et al. [1] omitted details of the real-time, windowed computation, making it difficult to understand precisely when ${}^{w}\mathcal{K}$ is updated. If it is computed at the end of any given fixation, then $\mathcal{K}$ would only be updated whenever a transition from fixation to saccade is detected. Instead of this presumed approach, $\mathcal{K}$ can be implemented so that it is updated with the arrival of the next raw gaze point, making its computation continuous in comparison to the presumed per-fixation approach of Abeysinghe et al.

In contrast to a windowed approach, instantaneous update of $\mathcal{K}$ relies on updating the current estimate of fixation duration, $\bar{d}$, or saccade amplitude, $\bar{a}$,

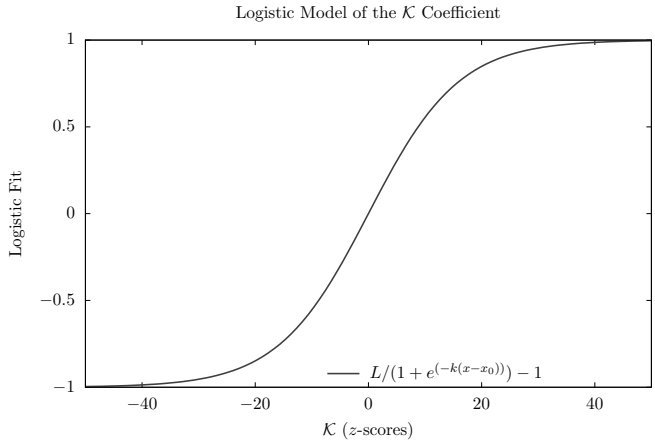

Fig. 2: Logistic function used to "squash" $\mathcal{K}$, with $L=2$ and $k=.125$. Note that this preserves $\mathcal{K}$'s response to $[-1:1]$ centering on 0 while dampening extreme values.

depending on the classification of the current gaze point, g_i, as shown in Fig. 1 and expressed in Eq. (3),

$$\mathcal{K}_i = \frac{\bar{d} - \mu_d}{\sigma_d} - \frac{\bar{a} - \mu_a}{\sigma_a} \tag{3}$$

which is similar to Eq. (1) save for the duration and amplitude accumulators. These are used to continuously expand on the current fixation's duration or the current saccade amplitude's distance, depending on the current gaze point's classification. In the present situation, a simple (I-VT) velocity-based classified is used by employing the Savitzky-Golay filter to obtain the velocity of the most recent point buffer (maintained by the filter) when the current gaze point g_i is added to the filter. In practice, two filters are used, one for each of the x- and y-components of the (2D) gaze position.

Moreover, evaluation of the current point as either a fixation or saccade will trigger one of the following four state transitions: saccade-saccade, saccade-fixation, fixation-fixation, fixation-saccade. If the transition is regressive (i.e., saccade-saccade or fixation-fixation) then the appropriate means and variance are updated.

In the case of a saccade-saccade transition, $\bar{a}$ is updated by accumulating the difference (amplitude) of the current point g_i and the most recent point (since it must also be a point that had been classified as a saccade). In the case of a fixation-fixation transition $\bar{d}$ is updated by accumulating the difference in timestamps of g_i and the most recent point since the latter would have been classified as part of a fixation.

In the case of transition from fixation to saccade, $\bar{d}$ is added to the duration ring buffer and reset to 0. Similarly, in the case of transition from saccade to fixation, $\bar{a}$ is appended to the amplitude ring buffer and then reset to 0.

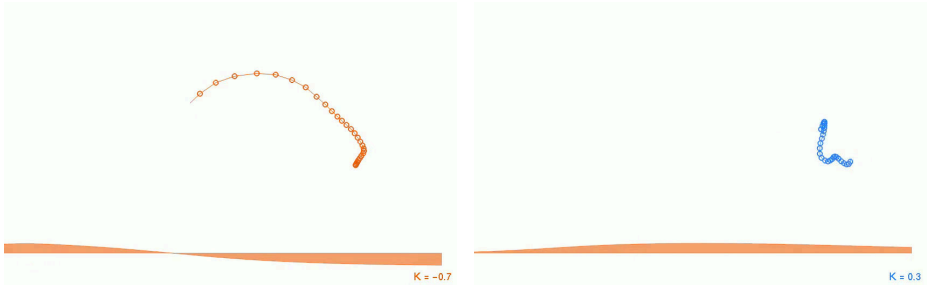

(a) Ambient movement consisting largely of saccadic gaze points transitioning from a fixation, $\mathcal{K} = -0.7$.

(b) Focal movement consisting largely of fixational gaze points transitioning from a saccade, $\mathcal{K} = 0.3$.

Fig. 3: Screen captures of simulation showing buffered gaze eye movements classified into saccades or fixations and real-time visualization of $\mathcal{K}$ displayed as a smoothed sinusoid, inspired by RealEye (http://realeye.io) sp, z.o.o.

Note that $\mathcal{K}$ as defined above is unbounded. For example, assume a fixation of infinite duration. Without an end to the fixation, $\bar{d}$ tends to infinity and thus also drives $\mathcal{K}$ to infinity. Similarly, a continuous saccade that never ends tends $\bar{a}$ to infinity and thus drives $\mathcal{K}$ to negative infinity. To mitigate this situation and to normalize $\mathcal{K}$, the logistic function $L/(1+e^{-kx})$ can be used to bound $\mathcal{K}$ to the $[-1:1]$ range as is often done in neural networks by "squashing" *activation functions* [7]. To do so, set $L = 2$, the supremum of the values of the function to set the range between asymptotes to $[-1:1]$. The choice of k is important here as it determines the logistic growth rate or steepness of the curve (bounding input values $x = \mathcal{K}_i$ over a shorter or wider range). A reasonable choice is $k = .125$ yielding the function shown in Fig. 2. Real-time behavior of $\mathcal{K}$ in a simulation of gaze is shown in Fig. 3, where $\mathcal{K}$ continuously varies between the $[-1:1]$ bounds in response to focal/ambient (simulated) eye movement, as expected.

2.2 Gaze Entropy

Given a set of Areas Of Interest (AOIs) $\mathcal{S} = \{1, \ldots, s\}$, with $s = |\mathcal{S}|$ denoting their number, gaze transition entropy is given by Eq. (4),

$$H_t = -\frac{1}{\log_2 s} \sum_{i \in \mathcal{S}} p_i \sum_{j \in \mathcal{S}} p_{ij} \log_2 p_{ij} \tag{4}$$

where p_i is the simple probability of viewing the i^{th} AOI (i.e., $1/s$), p_{ij} is the conditional probability of viewing the j^{th} AOI given the previous viewing of the i^{th} AOI, i.e., transitioning from the i^{th} to the j^{th} AOI. Transition entropy H_t provides a measure of statistical dependency in the spatial pattern of gaze represented by the transition matrix, $\mathbf{P} = (p_{ij})_{s \times s}$, which, in turn, is constructed from a sequence $\mathbf{x} = (x_0, \ldots, x_i, x_{i+1}, \ldots, x_n)$ of observed fixated (or simply glanced) AOIs, where $x_i \in \mathcal{S}$. The observed probability of gaze transition p_{ij} is

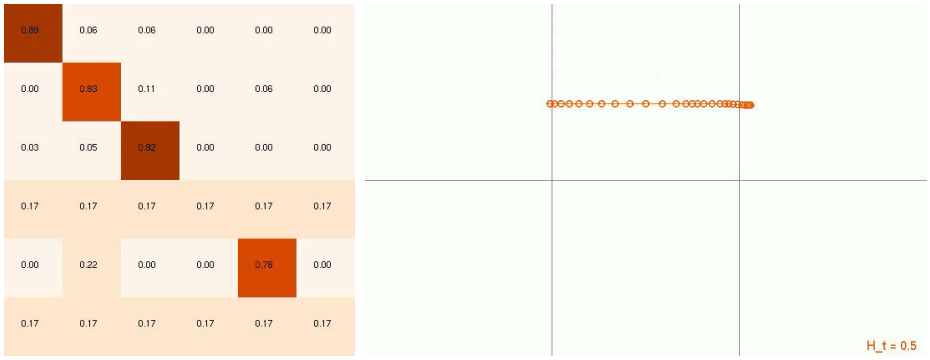

(a) Relatively high entropy, $H_t = 0.5$, when it should be lower since transitions are largely confined to only a subset of AOIs.

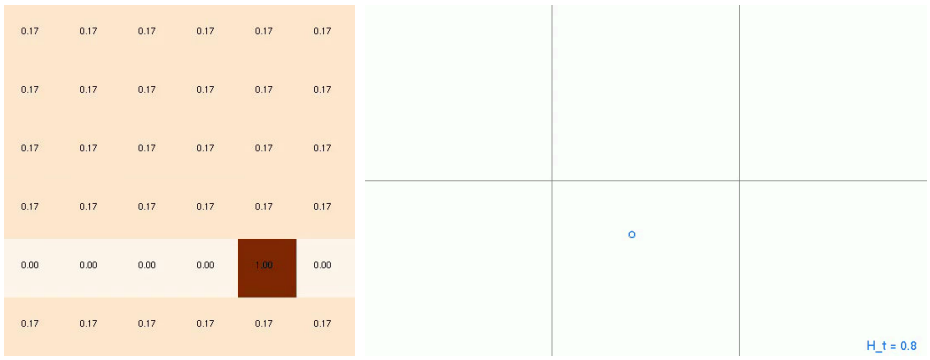

(b) Near maximum entropy, $H_t = 0.8$, since most transitions are equally likely although gaze is largely confined to a single AOI. In this case entropy should be 0.

Fig. 4: Screen captures of eye movement simulation over a 3×2 grid, with transition matrix at left with observed (instantaneous) transition probabilities between AOIs and grid at right with buffered simulated gaze. These screen captures serve to expose the inadequacy of the uniform distribution in the normalization assumption used by Krejtz et al. [12] which results in a counter-intuitive estimation of gaze entropy. See Sec. 2.3 for an improved reformulation of entropy that corrects this problem.

simply obtained by examining the transition between x_i, x_{i+1} in the sequence and accumulating the observation in transition matrix $\mathbf{P}$ at the appropriate matrix position.

As noted by Krejtz et al. [12], maximum entropy equal to $\log_2 s$ is reached when the distribution of transitions is uniform for each AOI. Minimal entropy of 0 describes a fully deterministic Markov chain. The higher the entropy, the more randomness there is in the viewing transitions. A good way to intuitively interpret entropy is to consider it as "expected surprise" of a given transition. Minimum entropy of 0 implies no surprise, while maximum entropy suggest maximum surprise. The term $-p_{ij} \log_2 p_{ij}$ in Eq. (4) is formally known as the *surprisal* [8].

Krejtz et al. [12] used gaze entropy as a means of comparison of one transition matrix to another. This has often been done where a transition matrix represented gaze transitions over a set of AOIs during a given experimental trial, thus allowing comparison of H_t between trials. Other variations allow similar comparisons but between user groups, where H_t can be used to compare gaze patterns between, for example, expert and novice pilots [2].

Note that entropy is generally tied to AOIs pre-defined in the scene. In the case of expert and novice pilots [2], AOIs can be defined over the instrument panel, front window, etc. This is the typical *context-sensitive* setup which relies on careful consideration of AOI placement and their dimensions (e.g., if they are not of uniform size, larger AOIs may be prone to drawing a greater proportion of gaze simply due to their size, relative to smaller AOIs). However, a *context-free* approach can also be considered if the user's gaze dispersion is of primary interest, irrespective of what is in the scene. This can be accomplished by specifying a virtual (uniform) grid of AOI cells in front of the user and then computing transitions between them.

Real-time implementation of gaze entropy relies on the choice of when to update the transition matrix and when to compute entropy from the matrix. Updating the matrix, in turn, relies on its initialization (during every update) and then its subsequent accumulation of observed probabilities of AOI transitions. These are maintained as a list (buffer) of recently visited AOIs. Note that the larger this buffer, the longer the system "memory". Hence, the buffer size is a user-adjustable parameter which will affect how quickly H_t changes in response to observed transitions. Currently, this is set to 125 with the number of AOIs set to an arbitrarily-sized $m \times n$ grid. If the number of AOIs is manageable (e.g., 4–12), matrix update and computation of H_t can be done fairly quickly allowing real-time performance.

As with computation of $\mathcal{K}$, H_t is sensitive to when it is performed, i.e., during which state transition. Currently, the sequence of visited AOIs is updated given every transition except saccade $\rightarrow$ saccade. Fig. 4 shows real-time eye movement simulation with both the real-time transition matrix and H_t.

Notice that H_t is artificially inflated, e.g., few or even no transitions yield large entropy. This results in a counter-intuitive interpretation of H_t and is due to the assumption made in constructing the transition matrix, namely in the instance when no transitions are observed from some given AOI to any other. In this instance, the gaze transition observations are imputed to $1/|\mathcal{S}|$ yielding equally likely probability transition from the AOI to any other. This uncertainty, if observed in many AOIs, will lead to an inflated entropy estimate. Below, this problem is addressed and a corrected version of gaze entropy is proposed.

2.3 Corrected Gaze Entropy Computation

Krejtz et al.'s [12] original formulation for gaze entropy computation employs entropy normalization, namely the division of $p_{ij}/\log_2 s$ found in Eq. (4). In the event of no observed transitions for any given AOI, its row entries in the transition matrix were set to $1/s$. Originally this was done to prevent matrix row sum

(a) Zero entropy, $H_t = 0.0$, with gaze fixed within a single AOI, yielding steady self-transitions, as it should be, since no transitions between any other AOIs do not contribute towards entropy.

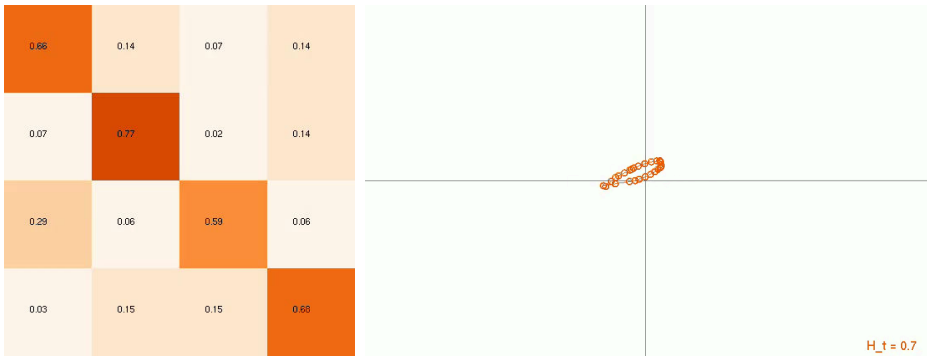

(b) High entropy, $H_t = 0.7$, as expected, since most transitions are almost as likely with gaze quickly moving between the AOIs, making it is difficult to predict the next AOI. There are no "empty" AOIs for which no transitions are observed.

Fig. 5: Screen captures of eye movement simulation over a 2×2 grid and corrected transition matrix at left with observed (instantaneous) transition probabilities between AOIs and grid at right with buffered simulated gaze.

division by zero. This is shown in Fig. 4(b) which results in a counter-intuitive estimation of gaze entropy when gaze is "stuck" in a specific AOI. This is because all other AOIs, for which no transition is actually observed, still assume equal probability of subsequent transitions. In the case of offline analysis, when generally most AOIs are eventually fixated over (relatively) long trials, these "empty" AOI transitions do not greatly influence the gaze entropy computation. However, in real-time implementation, "empty" AOIs tend to overpower the computation of the sole observed transition (self-transition within an AOI if the fixation is sufficiently long).

An improved reformulation of entropy computation that corrects this problem requires that:

1. AOIs for which no transitions are observed should not be counted,
2. normalization is adjusted to the number of AOIs for which transitions actually observed, and

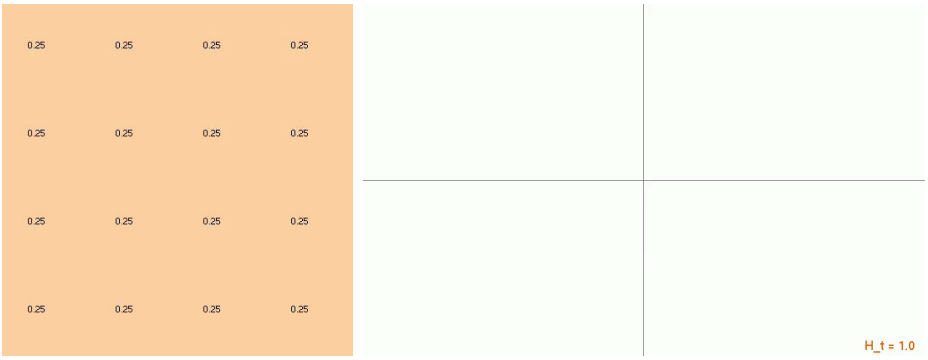

Fig. 6: Maximum entropy, $H_t = 1.0$, with gaze outside all AOIs. The normalization assumption used by Krejtz et al. [12] makes sense in this special case, leading to an intuitive estimation of entropy.

3. gaze entropy normalization introduced by Krejtz et al. [12] is preserved for the special case of transition matrix when gaze does not fall on *any* AOIs.

To handle the fist requirement, entries p_{ij} are set to 0 for any row in $\mathbf{P}$ which did not accumulate any observed transitions. In the computation of entropy, if a matrix row sums to 0, it will not be included in the entropy computation (preventing division by zero).

To handle the second requirement, the normalization factor of $\log_2 s$ is adjusted to $\log_2 \hat{s}$ where $\hat{s}$ is set to the number of non-zero sum rows of $\mathbf{P}$ instead of setting s to the number of AOIs, i.e., $s = |\mathcal{S}|$ as before.

Results of the implementation of these corrections are shown in Fig. 5. Notice that computation of H_t is now consistently intuitive, with zero entropy when gaze if fixed within a specific AOI, low entropy when gaze transitions between a few AOIs, and high entropy when gaze transitions among many AOIs.

Finally, in the special case of no observed transitions between any AOIs, i.e., all rows of $\mathbf{P}$ sum to zero, the imputation $p_{ij} = 1/\log_2 s, \forall i, j$ yields a uniformly distributed transition matrix $\mathbf{P}$ which results in maximum normalized entropy $H_t = 1$, as shown in Fig. 6.

3 Effects of User-Adjustable Parameters

There are only a few user-adjustable parameters that govern real-time computation of $\mathcal{K}$ and gaze entropy. Both metrics depend on the length of ring buffers used to store the recent history of sampled gaze points, $\mathcal{K}_i$ itself (mainly used for visualization rendering), and, for computation of gaze entropy, the sequence of observed AOIs. Ring buffers are realized through the use of double-ended queues. For both metrics, the length of the ring buffers, i.e., window size $w = 125$, produces reasonable behavior. The window size does not necessarily reflect a temporal window, since computation does not necessarily rely on completion of, say,

every 125 ms. However, assuming a sampling rate of 60 Hz, the window size can be thought of as $125 \times 1/60 \approx 2$ seconds worth of system memory. Manipulation of the window size will affect latency of metric computation.

For computation of $\mathcal{K}$, $k = 0.125$ is used in the logistic normalization and in this instance reflects what is considered a short sampling period of 125 ms, which, in turn, is based on the hypothesized 2-8 Hz environmental sampling conducted by the human attention network [3, 6].

For simulation of real-time computation of *context-free* gaze transition entropy, in addition to the window size ($w = 125$), a grid is used to denote AOIs with size ($m \times n$), currently set to $m = 3, n = 2$, yielding $m \times n$ number of AOIs, which requires an $mn \times mn$ transition matrix. As pointed out by Krejtz et al. [12], a more finely grained grid, with greater $m \times n$ dimensions yields diminishing returns. First, with a large number of AOIs, the estimate of entropy is drawn from a very sparse matrix, producing very low values of H_t. In this situation, stationary entropy H_s may be a more suitable estimate of entropy (see Krejtz et al. [12] for details). Second, the larger the transition matrix, the slower the computation.

4 Conclusion

Real-time implementation of gaze-based 2^{nd} order metrics, namely the $\mathcal{K}$ coefficient and gaze entropy H_t exposed inadequacies of their prior offline implementations, especially in the case of the latter. Key contributions of the derivation of real-time $\mathcal{K}$ and H_t include:

1. adjusting computation of $\mathcal{K}$ to instantaneously update the coefficient given real-time (x, y, t) gaze data without the need for a strictly temporally windowed approach, its normalization via the logistic function, and
2. correcting computation of H_t by removing an earlier design decision to impute the gaze transition matrix with uniform probability in the absence of observed transitions.

These innovations lead to fairly intuitive interpretations of simulated gaze. Future work is needed to validate both metrics via real-time controlled experiments. Moreover, since real-time implementations are sensitive to the length of the history buffer, such experimentation is needed to fine-tune user-adjustable parameters, e.g., grid dimension for context-free gaze entropy estimation and buffer length for real-time $\mathcal{K}$ responsiveness.

Both metrics are suitable for future *context-free* implementation in eye-tracking systems that do not rely on knowledge of the scene, e.g., as a means for gaze-based biometric measurement of gaze behavior.

References

1. Abeysinghe, Y., Mahanama, B., Jayawardena, G., Jayawardana, Y., Sunkara, M., Duchowski, A.T., Ashok, V., Jayarathna, S.: A-DisETrac Advanced Ana-

lytic Dashboard for Distributed Eye Tracking. International Journal of Multimedia Data Engineering and Management (IJMDEM) **15**(1), 1–20 (2024). https://doi.org/10.4018/IJMDEM.341792, http://doi.org/10.4018/IJMDEM.341792 1, 3

2. Ayala, N., Mardanbegi, D., Zafar, A., Niechwiej-Szwedo, E., Cao, S., Kearns, S., Irving, E., Duchowski, A.T.: Does fiducial marker visibility impact task performance and information processing in novice and low-time pilots? Computers & Graphics **119**, 103889 (2024). https://doi.org/https://doi.org/10.1016/j.cag.2024.103889, https://www.sciencedirect.com/science/article/pii/S0097849324000165 1, 7
3. Buschman, T.J., Kastner, S.: From Behavior to Neural Dynamics: An Integrated Theory of Attention. Neuron **88**(1), 127–144 (2015). https://doi.org/10.1016/j.neuron.2015.09.017, https://doi.org/10.1016/j.neuron.2015.09.017 10
4. Carbonell, I., de la Fuente, J., Afriyie, P.: Using Mobile Eye Tracking and Coefficient K for Analysing Usability Trials. In: Proceedings of the the 29th IAPRI Symposium on Packaging. pp. 345–357 (June 2019) 1
5. Duchowski, A.T., Krejtz, K.: Visualizing Dynamic Ambient/Focal Attention with Coefficient $\mathcal{K}$. In: Burch, M., Chuang, L., Fisher, B., Schmidt, A., Weiskopf, D. (eds.) Eye Tracking and Visualization: Foundations, Techniques, and Applications. ETVIS 2015, pp. 217–233. Springer International Publishing, Cham, Switzerland (2017). https://doi.org/10.1007/978-3-319-47024-5_13, http://dx.doi.org/10.1007/978-3-319-47024-5_13 1
6. Fiebelkorn, I.C., Kastner, S.: A Rhythmic Theory of Attention. Trends in Cognitive Sciences **23**(2), 87–101 (2019). https://doi.org/10.1016/j.tics.2018.11.009, https://doi.org/10.1016/j.tics.2018.11.009 10
7. Gershenfeld, N.A.: The Nature of Mathematical Modeling. Cambridge University Press, Cambridge, UK (1998) 5
8. Hume, E., Mailhot, F.: The Role of Entropy and Surprisal in Phonologization and Language Change. In: Yu, A.C.L. (ed.) Origins of Sound Change: Approaches to Phonologization, pp. 29–47. Oxford University Press, Oxford, UK (2013) 6
9. Just, M.A., Carpenter, P.A.: Eye Fixations and Cognitive Processes. Cognitive Psychology **8**(4), 441–480 (October 1976) 1
10. Karn, K.S.: "Saccade Pickers" vs. "Fixation Pickers": The Effect of Eye Tracker Choice on Research Findings (Panel Discussion). In: ETRA '00: Proceedings of the 2004 Symposium on Eye Tracking Research & Applications. pp. 87–88. ACM, New York, NY (2000) 2
11. Krejtz, K., Çöltekin, A., Duchowski, A.T., Niedzielska, A.: Using Coefficient $\mathcal{K}$ to Distinguish Ambient/Focal Visual Attention During Cartographics Tasks. Journal of Eye Movement Research **10(2)**(3), 1–13 (2017). https://doi.org/10.16910/jemr.10.2.3, http://dx.doi.org/10.16910/jemr.10.2.3 1
12. Krejtz, K., Duchowski, A., Szmidt, T., Krejtz, I., Perilli, F.G., Pires, A., Vilaro, A., Villalobos, N.: Gaze transition entropy. Transactions on Applied Perception **13**(1), 4:1–4:20 (Dec 2015). https://doi.org/10.1145/2834121, http://doi.acm.org/10.1145/2834121 1, 2, 6, 7, 9, 10
13. Krejtz, K., Duchowski, A.T., Krejtz, I., Szarkowska, A., Kopacz, A.: Discerning Ambient/Focal Attention with Coefficient $\mathcal{K}$. Transactions on Applied Perception **13**(3) (2016) 1, 2
14. Negi, S., Mitra, R.: Fixation duration and the learning process: an eye tracking study with subtitled videos. Journal of Eye Movement Research **13**(6) (2020), https://doi.org/10.16910/jemr.13.6.1 1

15. Salvucci, D.D., Goldberg, J.H.: Identifying Fixations and Saccades in Eye-Tracking Protocols. In: Eye Tracking Research & Applications (ETRA) Symposium. pp. 71–78. ACM, Palm Beach Gardens, FL (2000) 2
16. Savitzky, A., Golay, M.J.E.: Smoothing and differentiation of data by simplified least squares procedures. Analytical Chemistry **36**(8), 1627–1639 (1964), http://pubs.acs.org/doi/abs/10.1021/ac60214a047 2
17. Schafer, R.W.: What Is a Savitzky-Golay Filter? [Lecture Notes]. IEEE Signal Processing Magazing **28**(4), 111–117 (July 2011). https://doi.org/10.1109/MSP.2011.941097, http://dx.doi.org/10.1109/MSP.2011.941097 2
18. Warchoł-Jakubowska, A., Krejtz, K., Szczeciński, P., Wisiecka, K., Duchowski, A.T., Krejtz, I.: Visual Attention of Tram Drivers as a Step Towards Increasing Safety in Public Transport: A Comparative Eye-Tracking Study Between Novice and Expert Tram Drivers. Transport Problems **19**(1) (2024). https://doi.org/https://doi.org/10.20858/tp.2023.19.1.02 1